In Situ 13C and 23Na Magic Angle Spinning NMR Investigation of Supercritical CO2 Incorporation in Smectite–Natural Organic Matter Composites

ARTICLE *in* THE JOURNAL OF PHYSICAL CHEMISTRY C · FEBRUARY 2014

Impact Factor: 4.77 · DOI: 10.1021/jp410535d

6 AUTHORS, INCLUDING:

Geoffrey M. Bowers
Alfred University
21 PUBLICATIONS **201** CITATIONS
SEE PROFILE

David W Hoyt
Pacific Northwest National Laboratory
65 PUBLICATIONS **1,301** CITATIONS
SEE PROFILE

Sarah Burton
Pacific Northwest National Laboratory
68 PUBLICATIONS **1,459** CITATIONS
SEE PROFILE

Tamas Varga
Pacific Northwest National Laboratory
87 PUBLICATIONS **822** CITATIONS
SEE PROFILE

THE JOURNAL OF PHYSICAL CHEMISTRY C

Article

pubs.acs.org/JPCC

In Situ ^{13}C and ^{23}Na Magic Angle Spinning NMR Investigation of Supercritical CO_2 Incorporation in Smectite–Natural Organic Matter Composites

Geoffrey M. Bowers,*[,†] David W. Hoyt,[‡] Sarah D. Burton,[‡] Brennan O. Ferguson,[†] Tamas Varga,[‡] and R. James Kirkpatrick[§]

[†]Division of Chemistry, Alfred University, 1 Saxon Drive, Alfred, New York 14802, United States

[‡]William R. Wiley Environmental Molecular Sciences Laboratory, Pacific Northwest National Laboratory, Richland, Washington 99352, United States

[§]College of Natural Science, Michigan State University, East Lansing, Michigan 48824, United States

Supporting Information

ABSTRACT: This Article presents an in situ NMR study of clay–natural organic polymer systems (a hectorite–humic acid [HA] composite) under CO_2 storage reservoir conditions (90 bar CO_2 pressure, 50 °C). The ^{13}C and ^{23}Na NMR data show that supercritical CO_2 interacts more strongly with the composite than with the base clay and does not react to form other C-containing species over several days at elevated CO_2. With and without organic matter, the data suggest that CO_2 enters the interlayer space of Na–hectorite equilibrated at 43% relative humidity. The presence of supercritical CO_2 also leads to increased ^{23}Na signal intensity, reduced line width at half height, increased basal width, more rapid ^{23}Na T_1 relaxation rates, and a shift to more positive resonance frequencies. Larger changes are observed for the hectorite–HA composite than for the base clay. In light of recently reported MD simulations of other polymer–Na–smectite composites, we interpret the observed changes to be due to an increase in the rate of Na^+ site hopping in the presence of supercritical CO_2, the presence of potential new Na^+ sorption sites when the humic acid is present, and perhaps an accompanying increase in the number of Na^+ ions actively involved in site hopping. The results suggest that the presence of organic material either in clay interlayers or on external particle surfaces can significantly affect the behavior of supercritical CO_2 and the mobility of metal ions in clay-rich reservoir rocks.

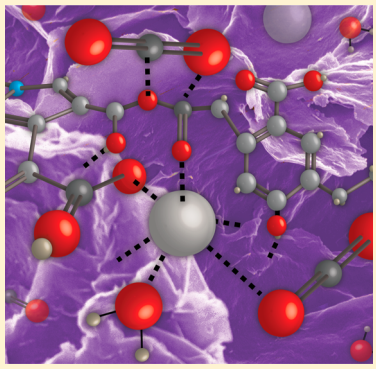

INTRODUCTION

There is currently great interest in the interaction of supercritical CO_2 (sCO_2) with rocks, minerals, and other geological fluids, largely as a result of the potential to mitigate atmospheric CO_2 levels using subsurface physical and chemical entrapment. Many studies in the past half-decade have improved our understanding of the fundamental molecular-scale structure, dynamics, and reactivity of ions and molecules at mineral–fluid interfaces under sCO_2 conditions. However, there is a substantial gap in our knowledge of how these behaviors change in the presence of naturally occurring organic matter, which is often associated with minerals in shales and other sedimentary rock types. Understanding reactivity as well as fluid and ion adsorption and dynamics in these complicated mineral–organo–H_2O–CO_2 systems is essential to predict the effectiveness of geological sequestration strategies and the long-term effects of sCO_2 on the geochemistry of subsurface aquifers, reservoir rocks, and minerals.

Clay minerals (smectites) make up a significant fraction of shales and other rocks in potential geological CO_2 repositories; thus, the interaction of these so-called "swelling clays" with sCO_2 on the molecular-scale has been an active area of research. Experimental[1−8] and molecular modeling[9−12] results for smectite–H_2O–CO_2 systems suggest that CO_2 can be incorporated into smectite interlayers at a variety of system H_2O contents, but also suggest that the amount of H_2O present affects the degree of CO_2 intercalation in smectite interlayers. For example, Botan et al.[9] used Monte Carlo (MC) computational methods to show that Na–montmorillonite with several different interlayer water contents preferentially incorporates CO_2 in its interlayer galleries relative to CO_2-saturated water at 75 °C and 25 and 125 bar, particularly in the one-layer hydrate where a monolayer of H_2O molecules is located in the smectite interlayer. Ilton et al.[4] observed similar results using in situ XRD with sCO_2 present. These results showed that sCO_2 enters the interlayer galleries of Na– and Ca–montmorillonites when even small amounts of H_2O are present and that the hydration state of the gallery (one-, two-, or three-layer hydrate) increases with increasing water saturation of the sCO_2. Giesting et al.[6,7] also used XRD to show CO_2 incorporation into the interlayers of hydrated Na–, K–, and Ca–montmorillonite, while Loring et al.[3] observed

Received: October 24, 2013
Revised: January 27, 2014
Published: January 29, 2014

   dx.doi.org/10.1021/jp410535d | J. Phys. Chem. C 2014, 118, 3564−3573

^{13}C NMR results consistent with CO_2 incorporation into the interlayers of one-layer hydrate smectites. Cygan et al.[10] demonstrated the stability of anhydrous CO_2–Na-montmorillonite complexes using a newly developed and highly accurate force field for MD and MC simulations of CO_2–clay systems. There are contradictory reports in the literature regarding the ability of CO_2 to react and form carbonate species that may ultimately trap CO_2 as carbonate minerals. On the basis of the XRD and ^{13}C NMR results mentioned above, Giesting et al.[6,7] proposed that interlayer CO_2 and H_2O can react to form carbonate species such as H_2CO_3 or HCO_3^-, whereas Loring et al.[3] found only one ^{13}C NMR resonance at the chemical shift of sCO_2 over the course of their in situ NMR experiments, demonstrating that carbonate species such as HCO_3^- are not formed under their experimental conditions.

Despite an improving molecular-scale understanding of smectite–H_2O–CO_2 interactions as a result of these studies, there is no published work examining binding, dynamics, and reactivity in smectite–organo–H_2O–CO_2 systems at sCO_2 conditions. In surface soils, the interaction of organic matter (OM) and minerals is thought to greatly affect the reactivity, chemical binding, transport, and availability of many species,[13−45] suggesting that OM will also play a crucial role in the fundamental surface chemistry under sCO_2 conditions. The only study involving smectite–organo–sCO_2 interactions of which we are aware is a recent MD computational investigation by Krishnan et al.[12] of anhydrous sCO_2 incorporation into the interlayer galleries of montmorillonite–(poly)ethylene glycol (PEG) composites. Their modeling results show that sCO_2 is stable in the interlayer galleries and that the sCO_2 interacts much more strongly with the PEG than with the clay surface. The results suggest that the presence of organic material in clay interlayers or on external clay surfaces may enhance CO_2 sorption at sCO_2 conditions relative to clay systems without organic material, both by opening the interlayer gallery and by providing additional adsorption sites. Krishnan and colleagues also show that charge-balancing Na^+ occurs on many types of sites in the montmorillonite–PEG composite material as compared to the base montmorillonite without PEG or sCO_2, that the Na^+ ions remain coordinated primarily by the smectite surface and ether oxygen atoms in the PEG molecules in the presence and absence of sCO_2, and that sCO_2 increases the rate of Na^+ site hopping in the clay–organo composite.[12]

Nuclear magnetic resonance (NMR) spectroscopy has several advantages over other molecular-scale spectroscopies capable of examining smectite–organo–H_2O–CO_2 systems, including element-specificity, sensitivity to light and heavy elements, and the ability to provide simultaneous structural and dynamical information over many time scales inaccessible by other techniques. Magic angle spinning (MAS) NMR is a well-established and highly effective method for improving understanding of the fundamental molecular-scale behaviors in geochemically relevant materials. Recent advances in high-pressure rotor design for MAS NMR[1,46] now allow acquisition of solid-state MAS NMR spectra at temperatures and pressures relevant to CO_2 sequestration,[1,3] offering an enormous opportunity to gain new insight into the fundamental geochemistry that occurs at mineral–organo–H_2O–CO_2 interfaces. This Article presents the results of an in situ high-pressure/high-temperature ^{13}C and ^{23}Na NMR study of sCO_2 interactions with the smectite clay, hectorite, with and without Suwannee River humic acid (HA). To our knowledge, this is the first NMR study of a hydrated smectite–organic system performed at elevated pressures and temperatures relevant to carbon sequestration and demonstrates that this approach can be useful to understanding the fundamental binding, dynamics, and reactivity in these complicated mineral–organo–H_2O–CO_2 systems. Our results show that under reservoir conditions CO_2 associates with the smectite–HA system, the CO_2–surface interactions are stronger in the system containing the HA, and that the CO_2 does not react to form inorganic C-bearing species. We also present evidence that sCO_2 causes changes in the interfacial behavior of the charge-balancing Na^+ leading to increased ion mobility and that the effects of sCO_2 on cation interfacial behavior are more significant in the system containing HA.

METHODS

Sample Synthesis. The base Na-saturated San Bernardino hectorite (available from the Clay Minerals Society) was prepared by placing 500 mg of the <2 μm fraction isolated and characterized previously[47,48] in 50 mL of 1 M NaCl solution in an 80 mL centrifuge tube, agitating the sample on a shaker table for 24 h, centrifuging the sample at 6000 rpm for 10 min, and decanting the supernatant solution. To remove residual NaCl, the sample was resuspended in deionized water and centrifuged. This rinse cycle was repeated three times. The sample was then freeze-dried, ground with an agate mortar and pestle, and sieved to <100 μm.

The Na–hectorite–HA composite was prepared using a procedure similar to that of Zhuang and Yu[49] involving the base Na–hectorite and as-received Suwannee River HA purchased from the International Humic Substance Society. To make the composite, 50 mg of the HA was dissolved in ∼30 mL of deionized water. 500 mg of the base Na hectorite was then added to the solution to make a suspension, which was established and maintained with a stir bar. The pH was monitored by a standard glass electrode. The suspension was titrated to a pH of ∼12 with 0.1 M NaOH and stirred for 30 min, then brought to a pH of ∼2.5 with 1.0 M HCl and equilibrated in a dark location while being stirred for 24 h to avoid potential photochemical reactions. After equilibration, the acidic suspension was transferred to an 80 mL centrifuge tube and centrifuged at 10 000 rpm (∼12 000g) for 10 min. The supernatant was decanted and the composite resuspended in deionized water and centrifuged. This rinse cycle was repeated twice, with the final supernatant appearing nearly colorless. After the final rinse, the composite was freeze-dried, ground, and sieved to <100 μm. All samples were stored in a desiccator over anhydrous P_2O_5 until they were later equilibrated for several days over K_2CO_3 saturated ^2H_2O (equivalent to 43% relative humidity, RH). For analysis, the hydrated samples were quickly transferred to the diffractometer or NMR rotor, and, in the case of the NMR analysis, were sealed against any moisture exchange with the atmosphere.

Sample Characterization. MicroXRD data for the samples were collected at the Environmental Molecular Sciences Laboratory (EMSL) at the Pacific Northwest National Laboratory (PNNL) using a Rigaku D/Max Rapid II instrument with a 2D image plate detector. X-rays were generated with a MicroMax 007HF generator fitted with a rotating Cr anode (λ = 2.2897 Å), and focused on the specimen through a 300 μm diameter collimator. Samples were dispersed on double-sided tape placed on the reflection holders. The data processing software 2DP (Ver. 1.0, Rigaku, 2007) was used to

dx.doi.org/10.1021/jp410535d | J. Phys. Chem. C 2014, 118, 3564−3573

integrate the diffraction rings captured by the 2-D image plate detector. Analysis of the diffraction data was carried out using JADE 9.5 (Materials Data, Inc.) and the PDF4+ 2012 database from ICDD. The pattern of Hectorite-16A, PDF# 9-0031, was matched to verify the presence of the hectorite and demonstrated the absence of other crystalline phases in the sample. Basal spacings were determined by fitting the diffraction peak for the (001) basal plane using a pseudo-Voigt profile function. The correct sample-to-detector distance was calibrated by measuring the lattice constant of a Si standard (silicon powder, NIST 640c). The observed lattice parameters deviated from the standard by 0.002 Å.

Both ^{23}Na and ^{13}C solid-state magic angle spinning (MAS) NMR experiments were performed at 50 °C at either atmospheric levels of CO_2 or 90 bar CO_2 (sCO_2) using a specialized 7.5 mm NMR rotor. The in situ high-pressure MAS NMR technique and apparatus for conducting mineral carbonation experiments has been described in detail previously.[1] The system includes a high-pressure MAS rotor (HP-MAS-R), which can be transferred to the spectrometers in a safety cell that keeps the loaded, pressurized rotor at 50 °C. The HP-MAS-R was loaded with 0.3 g of hectorite clay or the hectorite−HA composite equilibrated at 43% relative humidity and room temperature. These samples were then sealed, placed in an NMR probe, brought to 50 °C, and examined via ^{13}C and ^{23}Na Bloch-decay NMR. After acquisition of these baseline spectra, the rotor was preheated to 50 °C in the high-pressure gas loading apparatus in preparation for pressurization. The reaction chamber was evacuated to 1×10^{-3} Torr and purged with CO_2 gas three times for 5 min at each step prior to final pressurization of the sample. Research grade 99% ^{13}C labeled CO_2 gas (Sigma Aldrich - Isotech) was mixed with high-purity natural abundance CO_2 (OXARC) to obtain a ratio of 1:6, corresponding to a net isotope enrichment of ∼14.3%. The loading chamber containing the preheated rotor was then pressurized to 90 bar, and the rotor valve was opened. The clay sample was allowed to equilibrate in this environment for 1 h. The rotor was then sealed and transferred to the NMR laboratory to obtain ^{13}C and ^{23}Na MAS NMR spectra at 50 °C and spin rates of 3 ± 1 kHz. All ^{13}C NMR measurements were performed on an Agilent-Varian 300 MHz VNMRS spectrometer (H_0 = 7.05 T) at 75.44 MHz Larmor frequency using a Bloch-decay sequence with 31.2 kHz proton decoupling for 300 ms. All ^{13}C experiments employed a pulse width of 2 μs (45° flip angle) and used a relaxation delay of 5 s to acquire 120 transients. Spectra are referenced with respect to TMS via a secondary adamantane standard (37.85 ppm). The ^{13}C spectral width was 50 kHz, and 15 008 data points were acquired per transient. ^{23}Na NMR measurements were performed on a Varian-Chemagnetics 300 MHz Inova spectrometer at a Larmor frequency of 79.3 MHz using a 50 kHz spectral width. All ^{23}Na Bloch-decay and T_1 saturation-recovery experiments employed a pulse width of 1 μs ($\pi/20$ with respect to the solution) calibrated using 1 M NaCl (aq) and collected 2496 points in each of 1000 transients per 1D spectrum (one pulse) or element of the 2D time array (T_1 satrec). Bloch-decay data were recorded using a 1 s pulse delay between transients. The T_1 saturation-recovery experiments involved 75 pulses in the saturation train using a $\pi/2$ flip angle (3.5 μs pulse width) during the train and acquisition pulses, a 3 s delay between transients, and involved 20 different recovery delays between 250 μs and 40 s for the hectorite−HA composite and 20 delays between 10 μs and 5 s for the base Na−hectorite. The ^{23}Na NMR spectra were referenced with respect to 1 M NaCl (aq). All spectra were processed using custom NMR software written for Matlab/Octave and plotted using GNU plot. The ^{13}C NMR spectra were zero filled to a Fourier number of 32 000 points and given the equivalent of 5 Hz exponential apodization prior to taking the Fourier transform. For the ^{23}Na Bloch-decay experiments, the data sets were zero filled to 8192 data points, and 100 Hz of exponential apodization was applied before taking the FT. The ^{23}Na T_1 experiments were processed using iNMR (MestReC) and the same processing conditions, and the peak maxima and integrals were recorded. The T_1 data points were plotted versus the relaxation delay in the freeware program Abscissa (Rudiger Bruhl) and fit to a variety of T_1 functions.

RESULTS

Sample Characterization. The XRD patterns of the samples (Figure 1) show evidence that the HA is intimately associated with the Na−hectorite surfaces, likely within the interlayers and at the exterior of clay particles. The XRD pattern of the base Na−hectorite equilibrated at 43% relative humidity is essentially identical to that of the standard pattern and shows a basal spacing of 11.6 Å (∼10° 2θ), indicating that a vast majority of the interlayers contain the equivalent of 1 water layer.[50,51] The pattern of the hectorite−HA composite shows a basal spacing of 15.1 Å (8.7° 2 θ; identical to that of a two-layer hydrate without NOM) and also basal intensity extending to >35 Å (the low angles enclosed within the blue box), which is the low-angle limit for our diffractometer. Basal spacings larger than ∼15 Å must be due to expanded interlayers containing HA, because such spacings are never observed for hectorite samples held over the K_2CO_3−^2H_2O buffer without organic

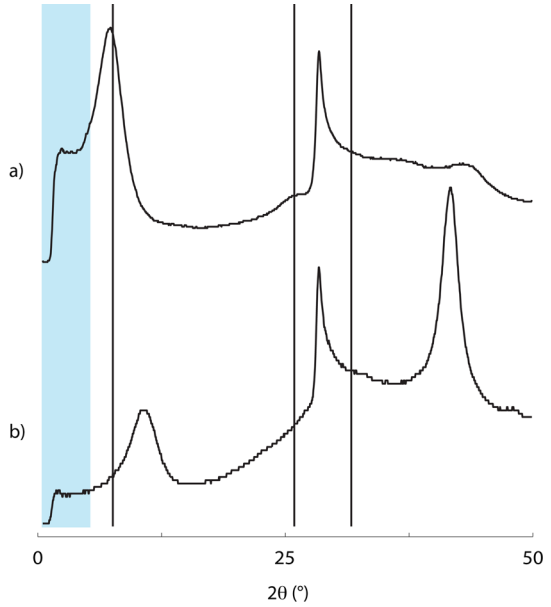

Figure 1. Powder X-ray diffraction patterns of (a) the Na−hectorite−HA composite and (b) the base Na−hectorite. The diffraction intensity at 2θ values less than ∼7° (upswing in intensity in the blue box) is likely due to expanded interlayer galleries containing HA. The origin of the additional intensity for the composite around the 26° and 33° 2θ range (marked with gray lines) is currently unclear, but these reflections are similar to XRD reflections observed in coals and may be due to HA external to the clay.

dx.doi.org/10.1021/jp410535d | J. Phys. Chem. C 2014, 118, 3564−3573

matter present.[50,52,53] The XRD pattern of the composite also shows a peak near 4.9 Å (~26° 2θ) and extra intensity near 3.5 Å (~33° 2θ) not present for the base Na–hectorite. The origin of these reflections is unclear at this time; however, we note that similar peaks have been observed in XRD patterns of coal samples and assigned to graphene-like stacking of aromatic regions (3.5 Å) and the spacing between aliphatic side-chains (5.0 Å).[54,55] This could be evidence of HA adopting an ordered structure adjacent to the smectite basal surfaces, but additional XRD studies of additional samples are necessary to fully support this conclusion. Electron/EDS microscopy of Na–hectorite coated with the full Suwannee River natural organic matter (rather than specifically the humic acid fraction) and subsequent simulation of the EDS interaction volume show that the organic matter coats the clay surfaces, sometimes to depths of more than 3 μm, suggesting that our samples have very thick coatings of humic acid on the external surface as compared to the typical clay platelet height (~7.6 Å) or interlayer spaces of one- or two-layer hydrates (2.5–5 Å).[56] The total H_2O content and distribution of H_2O in the Na–hectorite–HA sample were not determined, because the total amount of sample was small and it was saved for additional sCO_2 experiments. The likely hydration range in the Na–hectorite–HA spans from essentially H_2O-free HA-rich interlayers to ~1 to 1.2 H_2O/formula unit (that of a hectorite two-layer hydrate) prior to sCO_2 exposure.[51]

^{13}C and ^{23}Na NMR Spectra. The ^{13}C NMR spectra of the base Na–hectorite and the hectorite–HA composite consist of single resonances with maxima at 124.6 ± 0.2 ppm, the same value as for bulk sCO_2 (Figure 2). In both cases, only the $^{13}CO_2$ is observed because the ^{13}C in the HA is present at natural abundance and does not generate significant spectral intensity under these experimental conditions. The absence of resonances for other C-containing species formed by reaction of CO_2 with H_2O or the clay sheets demonstrates that the CO_2 has not reacted appreciably in these systems under our experimental conditions. The ^{13}C resonance for HCO_3^-, for instance, would appear near 161 ppm. However, the widths of the ^{13}C resonances for CO_2 increase from 11.3 Hz (full width at half height, fwhh) for sCO_2 alone to 18 Hz for the base Na–hectorite and 21.4 Hz for the composite. While several possible mechanisms may be responsible for this line broadening (see discussion below), the changes are very likely a result of interactions between the CO_2 molecules and the solid phase (clay or clay+HA). Line broadening of NMR resonances for fluids or for solutes in a fluid when fluid–surface interactions take place has long been observed in aqueous systems, and CO_2–surface interactions have been used previously to explain ^{13}C line broadening for a sCO_2–mineral system.[3]

The ^{23}Na MAS NMR spectra of our samples consist of single resonances with peak maxima between −28 and −21 ppm, along with poorly resolved spinning sidebands near 20 and −70 ppm (Figure 3). For the base Na–hectorite with and without sCO_2, the resonances are Gaussian in shape, indicative of a distribution of local chemical environments leading to dispersion of the chemical shielding and/or quadrupolar interactions.[50] The presence of sCO_2 has almost no influence on the ^{23}Na peak maximum of this sample (−23.5 ± 0.5 ppm without sCO_2 versus −22.8 ± 0.5 ppm with sCO_2), but does increase the peak area by ~23% and decrease the fwhh by ~1.7 ppm despite an increasing basal width. In contrast, the ^{23}Na resonances of the Na–hectorite–HA composite with and without sCO_2 are more asymmetric in shape with tails toward lower resonance frequencies, as is often observed for quadrupolar nuclei such as ^{23}Na in disordered solids. The

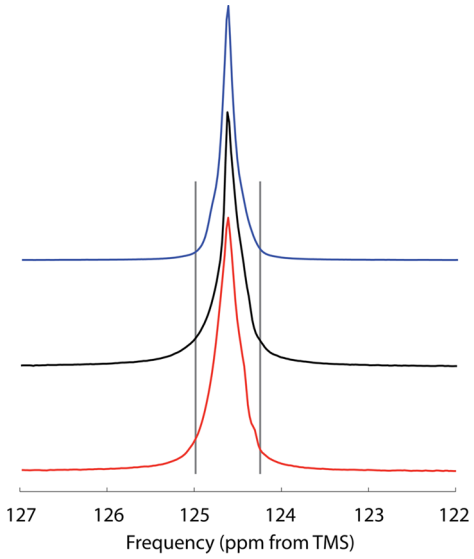

Figure 2. ^{13}C MAS NMR spectra of sCO_2 (blue), the base Na–hectorite (black), and the Na–hectorite–HA composite (red) obtained in situ at a CO_2 pressure of 90 bar and a temperature of 50 °C. The maximum peak intensities in each sample have been set to a value of 1 to highlight variations in the peak widths. The peak positions are the same in all spectra, demonstrating no reaction of CO_2 to form other species. The peak widths increase from sCO_2 to the base Na–hectorite to the composite, demonstrating CO_2 interaction with the solids and greater interaction in the presence of HA. For example, the increased basal widths are visible as increased intensity outside the gray vertical lines that mark the basal boundaries of the pure sCO_2 resonance. The asymmetric peak shape reflects the residual inhomogeneity in the magnetic field after shimming, as the line widths here are on the order of 20 Hz.

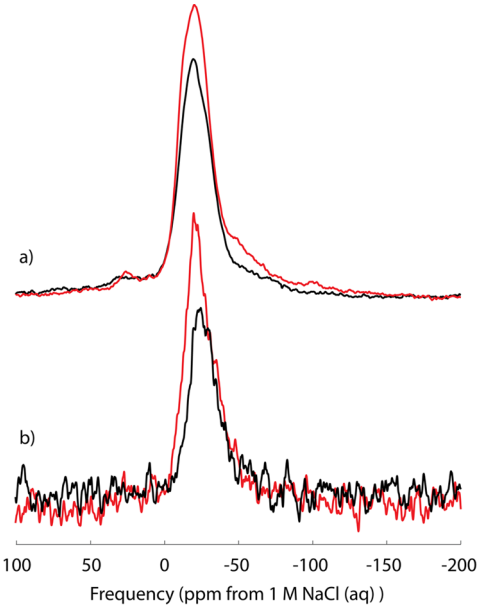

Figure 3. ^{23}Na MAS NMR spectra of (a) the base Na–hectorite and (b) the hectorite–HA composite, both at 50 °C with no CO_2 present (black) and at 50 °C and a CO_2 pressure of 90 bar (red). Spectra are plotted at their raw intensities and are directly comparable for the individual samples pre/post-sCO_2 exposure because the rotors were not unpacked between experiments. See text for discussion.

dx.doi.org/10.1021/jp410535d | J. Phys. Chem. C 2014, 118, 3564–3573

Table 1. ^{23}Na T_1 Relaxation Times (ms) from Our Best T_1 Analysis (Two Unique T_1 Components) for the Base Hectorite and Hectorite−Humic Acid (HA) Composite with and without sCO_2 Present

sample/T_1 component	p_{atm} CO_2, 50 °C[a]	90 bar CO_2, 50 °C	χ^2, p_{atm}	χ^2, 90 bar CO_2
base hectorite, short	4.0 ± 0.2	1.7 ± 0.1	1.733	1.190
base hectorite, long	330 ± 40	240 ± 30		
hectorite−HA composite, short	20 ± 15 (90 ± 14)	6.0 ± 1.5	12.58	1.64
hectorite−HA composite, long	240 ± 70 (2800 ± 1400)	380 ± 40		

[a]The values in parentheses for the composite are fits where two data points that do not fall on typical relaxation relationships are removed.

presence of sCO_2 also changes the peak maximum, in this case substantially: the observed maximum varies from −27 ± 1 ppm at atmospheric abundance of CO_2 to −21 ± 1 ppm with sCO_2 at 90 bar. As for the base hectorite, the presence of sCO_2 increases the peak area by ∼30% and decreases the fwhh by ∼1 ppm, while the width of the peak base increases. The two spectra for the composite are both noisier than those of the base Na−hectorite, as expected due to the decrease in the number of ^{23}Na spins as a result of dilution by the HA. The absence of resolvable features in the ^{23}Na spectra prevents us from determining changes in the quadrupolar coupling constants and asymmetry parameters. Development of in situ high-pressure and -temperature rotor systems for use at higher H_0 magnetic fields and acquisition of ^{23}Na NMR spectra for these samples will likely help increase resolution and allow evaluation of the second-order quadrupolar interaction's contribution to the line widths.[50] Because the interlayers and surfaces of smectite clays are highly disordered, it is unlikely that multiple quantum (MQMAS) NMR experiments will provide more information about the ^{23}Na quadrupolar interactions than multiple field studies.

^{23}Na T_1 Relaxation Experiments. The ^{23}Na T_1 relaxation results show that both HA and sCO_2 cause significant changes in the T_1 relaxation times ($1/T_1$ = relaxation rate) for our samples (Table 1). The data are well-fit with a two component saturation-recovery T_1 model that includes independent parameters for the amplitude of each component and identical saturation efficiencies (Supporting Information Figures S1, S2). Attempts to fit the data with stretched exponential functions were not successful, suggesting that there are truly two unique T_1 components in all of the samples rather than a continuous distribution of ^{23}Na T_1 values. The short component has T_1 values of the order of 10^0−10^1 ms. For both the base hectorite and the composite, the presence of sCO_2 causes the value of the short component to decrease, whereas the presence of humic acid results in longer T_1 values as compared to the base hectorite at both levels of system CO_2. The longer T_1 component has values of the order of 10^2 ms. The longer T_1 values for the base Na−hectorite and the composite without sCO_2 are statistically the same. With sCO_2 present, the T_1 value of this component is larger for the composite than for the base hectorite. However, we note that two of the data points for the composite sample in the absence of sCO_2 are located well off the typical shape of a T_1 curve, leading to the large values of uncertainties in this set of T_1 results (Table 1, Supporting Information Figure S2). With those two data points removed, the T_1 values for this sample increase substantially to 90.1 ± 14.2 ms for the short component and 2.78 ± 1.38 s for the long component, and the percent of ^{23}Na associated with each component changes dramatically (the fraction of ^{23}Na associated with the long T_1 time ranges from 70% to 27% for the full fit and that where the two points are removed, respectively). For the base Na−hectorite, the short component represents 70% of the total Na^+ in the sample and the long component 30% based on the fit amplitudes, more similar to the composite data when the two data points are removed. The relative abundance of the two Na^+ dynamic domains is unchanged for the base Na−hectorite by sCO_2, but the presence of sCO_2 does change these data for the composite sample such that ∼50% of ^{23}Na is associated with the short and the long T_1 component at 90 bar CO_2 and 50 °C.

DISCUSSION

sCO_2 Behavior in Na−Hectorite and Na−Hectorite/Humic Acid Composite. The ^{13}C and ^{23}Na NMR data are consistent with significant, direct molecular-scale sCO_2 interaction with the hectorite and hectorite−HA composite that increases in the presence of HA. They suggest that, at the very least, HA provides little barrier to the uptake of CO_2 into the interlayer galleries or onto exterior particle surfaces as compared to the one-layer hydrate of Na−hectorite and that humic acid may increase the CO_2 uptake relative to the HA-free system. For the base hectorite, the ^{13}C NMR results and interpretation in this work are essentially identical to those of Loring et al.[3] for montmorillonite (another smectite clay) immersed in supercritical $^{13}CO_2$. The increase in the ^{13}C NMR line width in the presence of the hectorite and the even greater increase for the hectorite−HA composite with respect to pure sCO_2 indicate increased CO_2−surface interactions. As noted above, line width increases of this type are often observed for systems containing liquids or gases interacting with macromolecules, large molecular clusters, and mineral surfaces. The increases occur because direct interaction of the observed fluid species with the solid decreases the fluid molecule's rate of motion and changes its instantaneous structural environment (and chemical shift) when it is in a surface sorption site. However, when fluid molecules have short residence times on these sites such that every molecule spends a majority of the millisecond NMR time scale in a bulk fluid environment, there is a single, narrow peak much like that for the bulk fluid but with increased line widths reflecting the modified, time-averaged molecular environment with respect to the bulk fluid due to the brief surface associations, as we observe in our data. The broader peak for the hectorite−HA composite indicates either a greater reduction in the rate of motion of proximity-restricted CO_2 (that within 5 Å of a surface), a greater residence time on the available binding sites, or the sampling of more diverse chemical environments when the humic acid is present. All of these explanations are consistent with the more complex interfacial structure we anticipate in the hectorite−HA composite as compared to the 2D siloxane sheets of the base hectorite. Separate resonances are not observed for different surface and bulk fluid sites in either system, because the site exchange (so-called diffusional averaging) occurs rapidly on the millisecond time scale of the NMR experiment at these temperatures and pressures.[48,49] In

dx.doi.org/10.1021/jp410535d | J. Phys. Chem. C 2014, 118, 3564−3573

principle, a more detailed test of the exchange rate hypothesis can come from performing identical experiments at a lower temperature where individual resonances for the unique exchanging environments can be resolved. Unfortunately, achieving a low enough temperature to accomplish this will probably take the sample out of the sCO_2 stability field.

Recent experimental[3−7] and computational molecular dynamics (MD) modeling[9−12] studies show that CO_2 enters and is stable in the interlayer galleries of smectite minerals and smectite−organo composites under supercritical conditions, suggesting that CO_2−organo interactions may be prevalent in geochemical systems. While there are many structural and chemical differences between HA and the synthetic polymers examined in these studies, NOM materials such as the Suwannee River HA used here do contain many oxygen-bearing functional groups (e.g., ethers, carbonyls, and carboxylic acids) that can coordinate to the C-atoms of CO_2 molecules (C_{CO2}). They also contain carbon atoms near electron-withdrawing groups where interactions between the O-atoms of CO_2 (O_{CO2}) and the partial positive charge on the C-atoms of HA can occur. Such interactions have been observed between CO_2 and PEG in MD modeling of the mutual interactions among montmorillonite, interlayer PEG, and interlayer CO_2.[12] These simulations show that for CO_2 the interaction with the polymer is much greater than with the clay surface and that this interaction occurs by coordination of the C_{CO2} by the ether oxygen atoms of the polymer and the O_{CO2} by the C-atoms of the polymer. Beyond the direct inner-sphere electrostatic CO_2−organo associations, protonated carboxylic acid groups and alcohols in the HA may also form hydrogen bonds with the O_{CO2} depending on the system pH, preparation conditions, and extent of hydration. On a macroscopic scale, the development of direct CO_2−HA interactions is also supported by the well-known fact that CO_2 interacts strongly with coal and readily displaces methane from it, although the molecular scale interactions and specific coordination environments of the CO_2−CH_4−coal system are not well understood.

Na^+ Binding and Dynamics in sCO_2−Na−Hectorite and sCO_2−Na−Hectorite−HA. Variations in the ^{23}Na peak maxima and widths in the presence of sCO_2 are likely the result of either static or dynamic reduction of the mean second-order quadrupolar interaction for ^{23}Na when sCO_2 is present. Focusing on the hectorite−HA composite where the effect of sCO_2 is more pronounced, the 6 ppm change in the observed chemical shift with sCO_2 versus atmospheric CO_2 could be the result of a new mean coordination environment with a different isotropic chemical shift, a reduced ^{23}Na second-order quadrupolar shift, or both. If the primary change were to the mean chemical shift, we would not expect to observe an increase in the integrated intensity of the resonance when sCO_2 is present if the number of ^{23}Na spins contributing to the resonance is constant, although the position and width could change. Our results show a substantial increase in the integrated intensity and the maintainance of a tailing, disordered quadrupolar-MAS line shape for the hectorite−HA composite at 90 bar CO_2, suggesting that sCO_2 stimulates a reduction in the second-order quadrupolar interaction. Such a reduction will shift intensity present in the satellite transitions of the low-pressure CO_2 system into the central transition peak that we observe in the composite, consistent with the increased peak area. This idea is also consistent with the direction of the change in chemical shift when 90 bar CO_2 is present in both the base hectorite and the composite, because the resonance moves toward the isotropic chemical shift of interlayer ^{23}Na in a dry base hectorite ($\sim -15.0 \pm 0.9$ ppm[50]), reflecting a reduced second-order quadrupolar shift. A reduced second-order quadrupolar shift and coupling constant implies a reduction in the electric field gradient (EFG) at the nucleus, which can be caused by a static increase in site symmetry, dynamical effects leading to increased time-averaged symmetry (such as occurs in fluids), or a combination of both effects. A reduction in the EFG via either mechanism will also lead to a decreased peak width and increased signal intensities, as we observe for the base hectorite and the hectorite−HA composite when sCO_2 is present. The increase in signal intensity for the composite in the presence of sCO_2 occurs principally on the high frequency side of the resonance, also as expected for reduction of the quadrupolar effects on the NMR resonance. With most data pointing toward a quadrupolar explanation for the ^{23}Na NMR behavior, the critical question becomes whether the ^{23}Na quadrupolar interaction is reduced in the presence of sCO_2 predominantly through static changes in the time-averaged binding environment symmetry or through dynamic time-averaged symmetry variations by more rapid hopping between binding sites that are structurally similar to those when sCO_2 is absent.

It seems likely that the observed effects of sCO_2 on the ^{23}Na NMR spectrum of the base hectorite are dominantly a result of increased dynamic averaging of the quadrupolar interaction rather than significant alterations to the dominant binding environment when sCO_2 is present. In the base hectorite, Na^+ occurs in the interlayer galleries and on exterior surfaces to provide charge balance for the negative structural charge of the clay T−O−T layers (see ref 51 for a recent review). Computational MD modeling of Na−montmorillonite shows that under supercritical conditions, CO_2 can coordinate Na^+ and can cause some Na^+ ions to be displaced from the surface and hop among several different local coordination environments.[9−11] While each of these coordination environments would be expected to have a different EFG, the CO_2 remains a component of individual Na^+ coordination shells for only brief transient periods on the nanosecond MD simulations. This suggests that the Na^+ environments in the Na−hectorite spend a majority of their time associated with the mineral surface on the millisecond time scales of our NMR experiments whether sCO_2 is present or not, and therefore that they should exhibit similar time-averaged ^{23}Na quadrupolar interactions unless the rate of Na^+ site hopping is altered by sCO_2. Thus, the observed ^{23}Na intensity increase in the sCO_2 system is most likely to be predominantly a result of a reduced time-averaged ^{23}Na quadrupolar interaction via a dynamic averaging mechanism.

It is not clear whether the substantially more negative ^{23}Na observed chemical shift for the composite sample with respect to the base hectorite is a result of a different mean coordination number and ^{23}Na isotropic chemical shift or an increased ^{23}Na quadrupolar interaction. As for CO_2, Na^+ in the composite can potentially occur in interlayer galleries with and without HA; at sites on hectorite particle external surfaces with and without HA present in the local, molecular scale environment; and displaced from the hectorite surface in thicker exterior or interlayer HA domains. Computational MD modeling of montmorillonite with interlayer PEG shows that the presence of the polymer can cause Na^+ to be displaced from the smectite surface and to be either partially or fully coordinated by the ether O-atoms of the PEG.[12] It is reasonable to expect that Na^+ may become displaced from the mineral surface in the

dx.doi.org/10.1021/jp410535d | J. Phys. Chem. C 2014, 118, 3564−3573

hectorite−HA composite and coordinate to ether O-atoms, carbonyl O-atoms, and deprotonated carboxylic acid and amine groups in the HA, and/or to develop complex mineral−H_2O−HA coordination environments involving protonated or deprotonated O-bearing or amine groups. Thus, there is likely to be a greater variety of Na^+ coordination environments in the composite sample as compared to the base hectorite. This conclusion is also consistent with the broad ^{23}Na NMR spectrum of a montmorillonite−PEG composite observed previously.[57] If the Na^+ sites in the composite have a larger mean coordination number, we would expect the ^{23}Na isotropic chemical shift to become more negative (analogous to the well-known differences between tetrahedral and octahedral Al), consistent with our ^{23}Na NMR results. However, it is also possible that the Na^+ sites have symmetries that lead to increased time-averaged ^{23}Na quadrupolar interactions, generating an increased second-order quadrupolar shift and moving the ^{23}Na peak maximum to a more negative observed shift. Additional characterization of the ^{23}Na quadrupolar interaction to resolve the relative influence of these two mechanisms will require similar experiments at a second H_0 field.

The observed changes in the ^{23}Na resonance of the composite when sCO_2 is present could also be a result of changing isotropic chemical shift or quadrupolar interactions, although it seems likely that dynamic averaging of the ^{23}Na second-order quadrupolar interactions is important in the composite samples as well. The MD results for the montmorillonite−PEG−CO_2 system, which is the only organo−smectite−CO_2 system that has been studied using MD methods, show that the Na^+ is coordinated predominantly to the oxygen atoms of the clay surface and the PEG but not significantly by the CO_2 at supercritical conditions, and that the Na^+ hops rapidly between coordination environments. Thus, these results suggest that the Na^+ coordination environments will be similar in the composite material with or without the presence of sCO_2 (as suggested for the HA-free system), making a reduction in the ^{23}Na isotropic chemical shift or the static ^{23}Na quadrupolar interaction of binding sites in the composite when sCO_2 is present unlikely. However, we do note that the distribution of Na^+ between the different types of sites could change and thereby affect the average chemical shift or quadrupolar interaction. Thus, the MD results suggest that sCO_2 will alter the ^{23}Na NMR predominantly by facilitating dynamic averaging of the ^{23}Na chemical quadrupolar interactions, and to a lesser extent the chemical shielding, via an indirect mechanism in which CO_2 is not part of the Na^+ coordination shell. One example of a possible indirect mechanism that facilitates more rapid dynamic averaging of the ^{23}Na NMR interactions is when CO_2 is incorporated into interlayer/surface HA and props open the HA structure, allowing the Na^+ more freedom to hop among sites. Thus, it seems likely that for both the base hectorite and the hectorite−HA composite, sCO_2-induced spectral variations are a result of an increased rate of Na^+ site hopping among similar types of binding environments, leading to a reduction in the time-averaged EFG due to dynamical effects.

The effects of HA and sCO_2 on the ^{23}Na T_1 relaxation times must also be due to dynamical processes, because for quadrupolar nuclei such as ^{23}Na changes in the T_1 relaxation pathway are predominantly a result of modulation of the ^{23}Na electric field gradient at the Larmor frequency (here 79.3 MHz). For solids, decreased T_1 relaxation times are normally due to increased rates of atomic motion, although we note that an increase in the dynamical power spectrum at the Larmor frequency due to a decrease in the rate of motion for very rapid processes will also produce reductions in T_1. The presence of two T_1 components here indicates the presence of two different types of Na^+ environments with different nanosecond-scale dynamical behaviors in all of the samples, irrespective of the presence of sCO_2 or HA. There are few other ^{23}Na T_1 data with which to compare our results. Our values are similar to those for ^{23}Na sorbed onto Illite, a phyllosilicate mineral with much higher structural charge than hectorite.[58] For Illite, the Na^+ is bound primarily on the exterior surfaces. Our observed T_1's are far too short to be due to unremoved, precipitated crystalline NaCl (^{23}Na T_1 = 11.5 s) or that reported for a Na-bearing polymer (^{23}Na T_1 of polyamide at 33% RH = 1.45 s), although there is little T_1 relaxation data for Na-polymers in general.[59]

For our samples, there are several possibilities for the different nanosecond dynamic environments. Na^+ could be on sites close to and far from paramagnetic centers such as impurity Fe or Mn, with those near the paramagnetic centers relaxing faster. Our hectorite, however, has a very low paramagnetic content, and paramagnetic relaxation via coupling to a small number of centers often leads to a continuous distribution of relaxation rates as opposed to the discrete values observed here. The continuous distribution for paramagnetic relaxation is related to the continuous distribution of distances between the observed spins and paramagnetic centers. The two T_1 components could also represent surface and interlayer sites, with Na^+ on exterior surfaces, perhaps, being the short component because they are less spatially constrained and thus more mobile. The larger relative magnitudes of the short T_1 component suggest that most of the ^{23}Na is associated with external surface Na^+. The two components could also be Na^+ on interlayer or surface sites with different amounts of water in their molecular environments, with those near more water molecules being more mobile and thus causing the short component. Surface sites, for instance, could have more adsorbed water. Additional NMR and neutron scattering experiments and computational modeling are needed to resolve this issue, although it seems likely that the two components are related in some way to the effects of water molecules.

Irrespective of the origin of the two T_1 components, for the base hectorite sCO_2 decreases both the short and the long T_1 values, indicating that it causes more rapid ^{23}Na relaxation and most likely increased rates of motion for both types of sites (Table 1). Similar effects on the NMR resonances of charge-balancing cations are observed for hydrous framework silicates due to increasing temperature.[60] For the composite, the best T_1 values show the same trend of sCO_2 causing smaller T_1's for the short T_1 component, but no significant trend in the longer component (Table 1). This may suggest that sCO_2 does not affect the second Na^+ dynamic population in the composite; however, we note that the hectorite−HA composite T_1 data at non-sCO_2 conditions come from the data set where two of the T_1 data points fall well outside the typical T_1 curve. By removing the two apparent outlier data points, the trend in the composite ^{23}Na T_1 values with sCO_2 present matches that of the base hectorite. The MD modeling of the montmorillonite−PEG−CO_2 system[12] shows that sCO_2 stimulates rapid Na^+ site hopping at frequencies >10^{10} Hz (fast enough to affect the T_1 behavior) with or without PEG in the interlayer. Although the composition and structure of HA are different than those of PEG, the modeling results strongly suggest that the observed changes in T_1 for our samples are due to dynamical effects

dx.doi.org/10.1021/jp410535d | J. Phys. Chem. C 2014, 118, 3564−3573

related to Na^+ site hopping, in agreement with our interpretations of the ^{23}Na signal intensity and line shape variations.

The relaxation results also show that the presence of HA causes longer T_1 values for both components in the hectorite−HA composite as compared to the base hectorite. This may be due to the HA affecting the amount and distribution of water in the sample or the rate/degrees of freedom for Na^+ motion. Quantitatively investigating the origin of the rate changes of the dynamical processes affecting ^{23}Na using NMR will require acquisition of spectra and T_1 data at multiple temperatures and fields when this capability is available, along with parallel computational modeling.

CONCLUSIONS

The in situ high-temperature and -pressure ^{13}C and ^{23}Na data for Na−hectorite and a Na−hectorite−humic acid composite presented here show that supercritical CO_2 can effectively interact with the clay and affect the behavior of Na^+ with or without organic matter present. Increases in ^{13}C peak widths with respect to bulk sCO_2 without an accompanying change in the observed chemical shift show interaction of CO_2 molecules with the solid phase without reaction of the CO_2 to form carbonate species under our experimental conditions. The increase is greater when humic acid is present, suggesting greater CO_2/solid phase interactions are stimulated by the presence of HA. Changes in the ^{23}Na spectra and T_1 relaxation rates show that both sCO_2 and natural organic matter affect the structural environments and dynamical behavior of charge balancing cations, with sCO_2 stimulating more rapid Na^+ site hopping.

The shales and other rocks present in potential geological C-sequestration sites contain clays and other minerals in intimate contact with complex natural organic matter, for which the hectorite−HA composite investigated here is a model material. The results show that understanding the effects of supercritical CO_2 injection into geological repositories will require investigation of not just the individual mineral components but the organic−inorganic composites. The differences in behavior of the minerals alone and the composite materials could lead to, for instance, differences in the sorption and release of CO_2, H_2O, cations, and hydrocarbons, and thus to different transport behaviors. Behavioral variations of organo−mineral composites could also lead to differences in the chemical reaction among these species and to the ways mineral precipitation occurs in these reservoirs. The results here combined with the results of recently published computational modeling studies show that NMR experiments under in situ supercritical CO_2 conditions can be effective in investigating critical, molecular scale interactions and dynamics in complex organic−inorganic systems.

ASSOCIATED CONTENT

Supporting Information

Plots of the ^{23}Na T_1 data sets and the associated fits. This material is available free of charge via the Internet at http://pubs.acs.org.

AUTHOR INFORMATION

Corresponding Author

*Phone: (607) 871-2822. E-mail: bowers@alfred.edu.

Notes

The authors declare no competing financial interest.

ACKNOWLEDGMENTS

This work was supported by the United States Department of Energy, Office of Basic Energy Science, through grants DE-FG02-10ER16128 and DE-FG02-08ER15929. The NMR spectra and microXRD data were obtained using facilities housed at the Environmental Molecular Sciences Laboratory, a national scientific user facility sponsored by the Department of Energy' s Office of Biological and Environmental Research and located at Pacific Northwest National Laboratory (PNNL). B.O.F. thanks the College of Liberal Arts and Sciences Dean's Office for funding to travel to PNNL.

REFERENCES

(1) Hoyt, D. W.; Turcu, R. V. F.; Sears, J. A.; Rosso, K. M.; Burton, S. D.; Felmy, A.; Hu, J. Z. High-Pressure Magic Angle Spinning Nuclear Magnetic Resonance. *J. Magn. Reson.* **2011**, *212*, 378−385.

(2) Felmy, A.; Qafoku, O.; Arey, B. W.; Hu, J. Z.; Hu, M.; Schaef, H. T.; Ilton, E. S.; Hess, N. J.; Pearce, C. I.; Feng, J.; Rosso, K. M. Reaction of Water-Saturated Supercritical CO_2 with Forsterite: Evidence for Magnesite Formation at Low Temperatures. *Geochim. Cosmochim. Acta* **2012**, *91*, 271−282.

(3) Loring, J. S.; Schaef, H. T.; Turcu, R. V. F.; Thompson, C. J.; Miller, Q. R. S.; Martin, P. F.; Hu, J.; Hoyt, D. W.; Qafoku, O.; Iton, E. S.; Felmy, A. R.; Rosso, K. M. In Situ Molecular Spectroscopic Evidence for CO_2 Intercalation into Montmorillonite in Supercritical Carbon Dioxide. *Langmuir* **2012**, *28*, 7125−7128.

(4) Ilton, E. S.; Schaef, H. T.; Qafoku, O.; Rosso, K. M.; Felmy, A. In Situ X-ray Diffraction Study of Na^+ Saturated Montmorillonite Exposed to Variably Wet Supercritical CO_2. *Environ. Sci. Technol.* **2012**, *46*, 4241−4248.

(5) Schaef, H. T.; Ilton, E. S.; Qafoku, O.; Martin, P. F.; Felmy, A.; Rosso, K. M. In situ XRD Study of Ca^{2+} Saturated Montmorillonite (STx-1) Exposed to Anhydrous and Wet Supercritical Carbon Dioxide. *Int. J. Greenhouse Gas Control* **2012**, *6*, 220−229.

(6) Giesting, P.; Guggenheim, S.; Koster van Groos, A. F.; Busch, A. Interaction of Carbon Dioxide with Na-Exchanged Montmorillonite at Pressures to 640 bar: Implications for CO_2 Sequestration. *Int. J. Greenhouse Gas Control* **2012**, *8*, 73−81.

(7) Giesting, P.; Guggenheim, S.; Koster van Groos, A. F.; Busch, A. X-ray Diffraction Study of K- and Ca-exchanged Montmorillonites in CO_2 Atmospheres. *Environ. Sci. Technol.* **2012**, *46*, 5623−5630.

(8) Miller, Q. R. S.; Thompson, C. J.; Loring, J. S.; Windisch, C. F.; Bowden, M. E.; Hoyt, D. W.; Hu, J. Z.; Arey, B. W.; Rosso, K. M.; Schaef, H. T. Insights into Silicate Carbonation Processes in Water-bearing Supercritical CO_2 Fluids. *Int. J. Greenhouse Gas Control* **2013**, *15*, 104−118.

(9) Botan, A.; Rotenberg, B.; Marry, V.; Turq, P.; Noetinger, B. Carbon Dioxide in Montmorillonite Clay Hydrates: Thermodynamics, Structure, and Transport from Molecular Simulation. *J. Phys. Chem. C* **2010**, *114*, 14962−14969.

(10) Cygan, R. T.; Romanov, V. N.; Myshakin, E. M. Molecular Simulation of Carbon Dioxide Capture by Montmorillonite Using an Accurate and Flexible Force Field. *J. Phys. Chem. C* **2012**, *116*, 13079−13091.

(11) Criscenti, L. J.; Cygan, R. T. Molecular Simulations of Carbon Dioxide and Water: Cation Solvation. *Environ. Sci. Technol.* **2013**, *47*, 87−94.

(12) Krishnan, M.; Saharay, M.; Kirkpatrick, R. J. Molecular Dynamics Modeling of CO_2 and (Poly)Ethylene Glycol in Montmorillonite: The Structure of Clay-Polymer Composites and the Incorporation of CO_2. *J. Phys. Chem. C* **2013**, *117*, 20592−20609.

(13) Bertsch, P. M.; Seaman, J. C. Characterization of Complex Mineral Assemblages: Implications for Contaminant Transport and

Environmental Remediation. *Proc. Natl. Acad. Sci. U.S.A.* **1999**, *96*, 3350−3357.
(14) Bailey, G. W.; Akim, L. G.; Shevchenko, S. M. Predicting Chemical Reactivity of Humic Substances for Minerals and Xenobiotics: Use of Computational Chemistry. *Scanning Probe Microsc., Virtual Reality* **2001**, 41−72.
(15) Dumat, C.; Staunton, S. Reduced Adsorption of Caesium on Clay Minerals Caused by Various Humic Substances. *J. Environ. Radioact.* **1999**, *46*, 187−200.
(16) Krishnamurti, G. S. R.; Naidu, R. Speciation and Phytoavailability of Cadmium in Selected Surface Soils of South Australia. *Aust. J. Soil Res.* **2000**, *38*, 991−1004.
(17) Lee, S. S.; Nagy, K. L.; Park, C.; Fenter, P. Enhanced Uptake and Modified Distribution of Mercury(II) by Fulvic Acid on the Muscovite (001) Surface. *Environ. Sci. Technol.* **2009**, *43*, 5295−5300.
(18) Murphy, E. M.; Zachara, J. M. The Role of Sorbed Humic Substances on the Distribution of Organic and Inorganic Contaminants in Groundwater. *Geoderma* **1995**, *67*, 103−124.
(19) Petrovic, M.; Kastelan-Macan, M.; Horvat, A. J. M. Interactive Sorption of Metal Ions and Humic Acids onto Mineral Particles. *Water, Air, Soil Pollut.* **1999**, *111*, 41−56.
(20) Zachara, J. M.; Resch, C. T.; Smith, S. C. Influence of Humic Substances on Co^{2+} Sorption by a Subsurface Mineral Separate and Its Mineralogic Components. *Geochim. Cosmochim. Acta* **1994**, *58*, 553−566.
(21) Chen, B.; Evans, J. R. G.; Greenwell, H. C.; Boulet, P.; Coveney, P. V.; Bowden, A. A.; Whiting, A. A Critical Appraisal of Polymer-Clay Nanocomposites. *Chem. Soc. Rev.* **2008**, *37*, 568−594.
(22) Schevchenko, S. M.; Bailey, G. W. Non-Bonded Organo-Mineral Interactions and Sorption of Organic Compounds on Soil Surfaces: A Model Approach. *J. Mol. Struct. (THEOCHEM)* **1998**, *422*, 259−270.
(23) Guo, M.; Chorover, J. Transport and Fractionation of Dissolved Organic Matter in Soil Columns. *Soil Sci.* **2003**, *168*, 108−118.
(24) Hernandez-Ruiz, S.; Abrell, L.; Wickramasekara, S.; Chefetz, B.; Chorover, J. Quantifying PPCP Interaction with Dissolved Organic Matter in Aqueous Solution- Combined Use of Fluorescence Quenching and Tandem Mass Spectrometry. *Water Res.* **2012**, *46*, 943−954.
(25) Kirishima, A.; Tanaka, K.; Niibori, Y.; Tochiyama, O. Complex Formation of Calcium with Humic Acid and Polyacrylic Acid. *Radiochim. Acta* **2002**, *90*, 555−561.
(26) Kubota, T.; Tochiyama, O.; Tanaka, K.; Niibori, Y. Complex Formation of Eu (III) with Humic Acid and Polyacrylic Acid. *Radiochim. Acta* **2002**, *2002*, 569−574.
(27) Lee, S. S.; Nagy, K. L.; Fenter, P. Distribution of Barium and Fulvic Acid at the Mica-Solution Interface Using in-situ X-ray Reflectivity. *Geochim. Cosmochim. Acta* **2007**, *71*, 5763−5781.
(28) Navon, R.; Hernandez-Ruiz, S.; Chorover, J.; Chefetz, B. Interactions of Carbamazepine in Soil: Effects of Dissolved Organic Matter. *J. Environ. Qual.* **2011**, *40*, 942−948.
(29) Piccolo, A. The Supramolecular Structure of Humic Substances: A Novel Understanding of Humus Chemistry and Implications in Soil Science. *Adv. Agron.* **2002**, *75*, 57.
(30) Sposito, G. *The Surface Chemistry of Soils*; Oxford University Press: New York, 1989.
(31) Stevenson, F. J. *Humus Chemistry: Genesis, Composition, Reactions*; John Wiley and Sons: New York, 1994.
(32) Wershaw, R. L. Evaluation of Conceptual Models of Natural Organic Matter (Humus) from a Consideration of the Chemical and Biochemical Processes of Humification. U.S. Geological Survey Scientific Investigations Report, 2004.
(33) Aquino, A. J. A.; Tunega, D.; Pasalic, H.; Haberhauer, G.; Gerzabek, M. H.; Lischka, H. The Thermodynamic Stability of Hydrogen Bonded and Cation Bridged Complexes of Humic Acid Models - A Theoretical Study. *Chem. Phys.* **2008**, *349*, 69−76.
(34) Borrok, D.; Aumend, K.; Fein, J. B. Significance of Ternary Bacteria-Metal-Natural Organic Matter Complexes Determined Through Experimentation and Chemical Equilibrium Modeling. *Chem. Geol.* **2007**, *238*, 44−62.
(35) Brigante, M.; Zanini, G.; Avena, M. On the Dissolution Kinetics of Humic Acid Particles. Effects of pH, Temperature und Ca^{2+} Concentration. *Colloids Surf., A* **2007**, *294*, 64−70.
(36) Kalinichev, A. G.; Iskrenova-Tchoukova, E.; Ahn, W.-Y.; Clark, M. M.; Kirkpatrick, R. J. Effects of Ca^{2+} on Supramolecular Aggregation of Natural Organic Matter in Aqueous Solutions: A Comparison of Molecular Modeling Approaches. *Geoderma* **2011**, *169*, 27−32.
(37) Kalinichev, A. G.; Kirkpatrick, R. J. Molecular Dynamics Simulation of Cationic Complexation with Natural Organic Matter. *Eur. J. Soil Sci.* **2007**, *58*, 909−917.
(38) Lee, S. S.; Fenter, P.; Park, C.; Nagy, K. L. Fulvic Acid Sorption on Muscovite Mica as a Function of pH and Time Using In Situ X-ray Reflectivity. *Langmuir* **2008**, *24*, 7817−7829.
(39) Lee, S. S.; Nagy, K. L.; Park, C.; Fenter, P. Heavy Metal Sorption at the Muscovite (001)-Fulvic Acid Interface. *Environ. Sci. Technol.* **2011**, *45*, 9574−9581.
(40) Wall, N. A.; Choppin, G. R. Humic Acids Coagulation: Influence of Divalent Cations. *Appl. Geochem.* **2003**, *18*, 1573−1582.
(41) Ahn, W.; Kalinichev, A. G.; Clark, M. M. Effects of Background Cations on the Fouling of Polyethersulfone Membranes by Natural Organic Matter: Experimental and Molecular Modeling Study. *J. Membr. Sci.* **2008**, *309*, 128−140.
(42) Iskrenova-Tchoukova, E.; Kalinichev, A. G.; Kirkpatrick, R. J. Metal Cation Complexation with Natural Organic Matter in Aqueous Solutions: Molecular Dynamics Simulations and Potentials of Mean Force. *Langmuir* **2010**, *26*, 15909−15919.
(43) Kalinichev, A. G. Molecular Models of Natural Organic Matter and Its Colloidal Aggregation in Aqueous Solutions: Challenges and Opportunities for Computer Simulations. *Pure Appl. Chem.* **2013**, *85*, 149−158.
(44) Leenheer, J. A. Systematic Approaches to Comprehensive Analyses of Natural Organic Matter. *Ann. Environ. Sci.* **2009**, *3*, 1−130.
(45) Parikh, S. J.; Chorover, J. ATR-FTIR Study of Lipopolysaccharides at Mineral Surfaces. *Colloids Surf., B* **2008**, *62*, 188−198.
(46) Turcu, R. V. F.; Hoyt, D. W.; Rosso, K. M.; Sears, J. A.; Loring, J. S.; Felmy, A.; Hu, J. Z. Rotor Design for High Pressure Magic Angle Spinning Nuclear Magnetic Resonance. *J. Magn. Reson.* **2013**, *226*, 64−69.
(47) Weiss, C. A.; Kirkpatrick, R. J.; Altaner, S. P. Variations in Interlayer Cation Sites of Clay-Minerals as Studied by Cs-133 MAS Nuclear-Magnetic-Resonance Spectroscopy. *Am. Mineral.* **1990**, *75*, 970−982.
(48) Weiss, C. A.; Kirkpatrick, R. J.; Altaner, S. P. The Structural Environments of Cations Adsorbed onto Clays - Cs-133 Variable-Temperature MAS NMR Spectroscopic Study of Hectorite. *Geochim. Cosmochim. Acta* **1990**, *54*, 1655−1669.
(49) Zhuang, J.; Yu, G.-R. Effects of Surface Coatings on Electrochemical Properties and Contaminant Sorption of Clay Minerals. *Chemosphere* **2002**, *49*, 619−628.
(50) Bowers, G. M.; Singer, J. W.; Bish, D. L.; Kirkpatrick, R. J. Alkali Metal and H_2O Dynamics at the Smectite/Water Interface. *J. Phys. Chem. C* **2011**, *115*, 23395−23407.
(51) Morrow, C. P.; Yazaydin, A. O.; Kalinichev, A. G.; Bowers, G. M.; Kirkpatrick, R. J. Structure and Dynamics of Clay Surfaces and Interlayers: Molecular Dynamics Investigations of Na-hectorite. *J. Phys. Chem. C* **2013**, *116*, 22987−22991.
(52) Bowers, G. M.; Bish, D. L.; Kirkpatrick, R. J. H_2O and Cation Structure and Dynamics in Expandable Clays: ^2H and ^{39}K NMR Investigations of Hectorite. *J. Phys. Chem. C* **2008**, *112*, 6430−6438.
(53) Bowers, G. M.; Singer, J. W.; Bish, D. L.; Kirkpatrick, R. J. Ion and H_2O Structure and Dynamics in the Interlayer of Na- and Ca-Hectorite. *Am. Mineral.*, in press.
(54) Lu, L.; Sahajwalla, V.; Kong, C.; Harris, D. Quantitative X-ray Diffraction Analysis and It Application to Various Coals. *Carbon* **2001**, *39*, 1821−1833.

(55) Takagi, H.; Maruyama, K.; Yoshizawa, N.; Yamada, Y.; Sato, Y. XRD Analysis of Carbon Stacking Structure in Coal During Heat Treatment. *Fuel* **2004**, *83*, 2427−2433.
(56) Kirkpatrick, R. J.; Ferguson, B. O.; Arey, B. W.; Varga, T.; Burton, S. D.; Bowden, M. E.; Dohnalkova, A.; Bowers, G. M. Unpublished data.
(57) Reinholdt, M. X.; Kirkpatrick, R. J.; Pinnavaia, T. J. Montmorillonite-Poly(ethylene Oxide) Nanocomposites: Interlayer Alkali Metal Behavior. *J. Phys. Chem. B* **2005**, *109*, 16296−16303.
(58) Kim, Y.; Kirkpatrick, R. J. NMR T-1 Relaxation Study of Cs-133 and Na-23 Adsorbed on Illite. *Am. Mineral.* **1998**, *83*, 661−665.
(59) Xu, X.; Kirkpatrick, R. J. NaCl Interaction with Interfacially Polymerized Polyamide Films of Reverse Osmosis Membranes: A Solid-State Na-23 NMR Study. *J. Membr. Sci.* **2006**, *280*, 226−233.
(60) Kim, Y.; Kirkpatrick, R. J. High-temperature Multinuclear NMR Investigation of Analcime. *Am. Mineral.* **1998**, *83*, 339−347.